Int J Clin Exp Med 2021;14(7):2141-2152
www.ijcem.com /ISSN:1940-5901/IJCEM0124341

Original Article

rhCygb benefits bleomycin-induced established pulmonary fibrosis in rats

Zhen Li[1*], Zhongshun Lin[1,2*], Ping Wang[1], Wenqi Dong[1]

[1]Laboratory Medicine and Biotechnology, Southern Medical University, Guangzhou 510515, Guangdong Province, PR China; [2]Jiangmen Central Hospital, Affiliated Jiangmen Hospital of Sun Yat-sen University, Jiangmen 529000, Guangdong Province, PR China. [*]Equal contributors and co-first authors.

Received October 17, 2020; Accepted May 27, 2021; Epub July 15, 2021; Published July 30, 2021

Abstract: Recombinant human cytoglobin (rhCygb) has been demonstrated to have anti-inflammatory, antioxidative, and antifibrotic effects in livers and kidneys in animal disease models. However, the effect of rhCygb on the progression of pulmonary fibrosis is still unclear. In this study, we investigated rhCygb's therapeutic effects on lung fibrosis in rats treated with bleomycin. Bleomycin (5 mg/kg) resulted in fibrosis that could be detected using CT and serum measurements at day 7. The effects of the rhCygb treatment on the morphological and CT imaging of the lungs, as well as the serial serum levels of the biomarkers with progressive lung fibrosis were tested at days 28 and 56. The results showed that evidence for well-established lung fibrosis was determined by the changes in the rat lungs using CT images and the serum HA, LN, PIIINP, and IVC levels at 7 days. After treatment with rhCygb for 49 days, we found significantly decreased and almost normal HA, LN, PIIINP, and IVC levels. The hydroxyproline, CT-MLD, and Masson CVF levels were also significantly reduced. Furthermore, the CT-MLD levels positively correlated with the serum HA, LN, PIIINP, IVC, and HYP levels, and especially with the CVF levels. Taken together, our data suggest that rhCygb is a potential new medicine for reversing lung fibrosis.

Keywords: Recombinant human cytoglobin, bleomycin, pulmonary fibrosis, computed tomography

Introduction

Idiopathic pulmonary fibrosis (IPF) is a rare but fatal lung disease, characterized by chronic alveolar walls and interstitial fibrosis in lung tissue, and causing a progressive decline in lung function and ultimately respiratory failure [1]. Most patients with IPF may also have pulmonary hypertension, emphysema, or obstructive sleep apnea; the estimated median survival time is 2-5 years following diagnosis [2]. Typical high-resolution computed tomography (HRCT) of the IPF displays fibrotic changes in both the basal and peripheral lungs, with reticular opacities, honeycomb changes, and ground-glass opacities [3]. Clinically, the morbidity and mortality of pulmonary fibrosis patients are very high, and the therapeutic effects of their drug treatments are limited [4]. Therefore, the development of an anti-fibrotic drug would fill an urgent clinical need.

An extracellular matrix (ECM) is a highly dynamic macromolecular structure that provides both three-dimensional tissues and functional support to organs [5]. In the lungs, the excessive extracellular matrix is generally composed of fibrillar proteins, glycoproteins, glycosaminoglycans, and the basement membrane laminin. There are still some variants of ECM constituents which have not been characterized [6]. The lung ECM is confined to contribute to health and disease; thus, serum ECM molecules have been used to evaluate the progression of fibrosis and patient prognosis [7, 8]. Yilang et al. found significantly higher serum levels of ECM molecules in IPF patients, involving laminin (LN), type IV collagen (IVC), procollagen III N-terminal peptide (PIIINP), and hyaluronic acid (HA), compared with healthy individuals. They pointed out that the serum LN, IVC, PIIINP, and HA levels might indicate IPF progression and might be indicators for the severity of IPF [9].

Cytoglobin (Cygb) is a member of the globin family, which was discovered in hepatic stellate cells in 2001 [10]. At that time, it was also found in several organs, such as the kidneys

and the pancreas, and it was found to be especially localized in fibroblast-like cells. In the past decade, Cygb was reported to be associated with many physiological functions, including the cytoprotection against oxidative and nitrosidative stress [11, 12], fibrotic stimulation [13-15], and tumor suppression [16-18]. Recombinant human cytoglobin (rhCygb) is a biologically synthesized protein. Our previous studies have shown that rhCygb can prevent atherosclerosis and protects against chronic liver disease and liver fibrosis [20-23]. These findings led to the hypothesis that rhCygb is effective in the treatment of lung fibrosis. Therefore, in this study, a BML-induced pulmonary fibrosis rat model was established to observe the effects of rhCygb on the pulmonary tissue and serum levels of the four ECM molecules (HA, LN, PIIINP, and IVC).

Material and methods

Experimental animals

Male rats (Sprague-Dawley, SD) with an average weight of 180-220 g were purchased from the Guangdong Medical Laboratory Animal Center, China. The animal care in this investigation was done according to the guidelines approved by the Chinese Association of Laboratory Animal Care. The rats were housed in groups of 5 per cage under a constant temperature (20±2°C) and humidity (70%) with a 12 h light-dark cycle, and they had free access to food and water. The animals were acclimatized for one week prior to the experiments. All the animal protocols were approved by the Ethics Committee for Animal Research of Southern Medical University.

To induce pulmonary fibrosis, the rats were anesthetized with 2% pentobarbital (50 mg/kg body weight) and placed on an intubation stand facing upward at an angle of approximately 30-35° using an elastic string carefully positioned under the animal's front incisors. The tongue was gently pulled out with forceps and the trachea was intubated. The BLM-treated rats were intratracheally instilled with 5 mg/kg bleomycin sulfate (Nippon Kayaku, Tokyo, Japan) solution in 0.9% saline as previously described [24], and slowly instilled through the catheter into the trachea. The control rats simultaneously received the same volume of 0.9% saline solution without bleomycin.

The SD rats were randomly allocated to the following groups: (1) SD rats receiving a single intratracheal instillation of saline solution and sacrificed after 56 days (n=11); (2) SD rats receiving a single intratracheal instillation of BLM (5 mg/kg) and sacrificed after 56 days (n=11); (3) SD rats receiving a single intratracheal instillation of BLM (5 mg/kg), and 7 days later, treated with rhCygb (4 mg/kg, daily, subcutaneously) for 49 days (n=12); (4) SD rats receiving a single intratracheal instillation of BLM (5 mg/kg), and 7 days later, treated with dexamethasone (DXMS) (3 mg/kg, daily, subcutaneously) for 49 days (n=11).

A general schedule of the treatment is shown in **Figure 1**. The rats were scanned with a multi-slice spiral CT at days 7 and 56. Finally, the rats were sacrificed, and specimens of their lungs were harvested and processed for subsequent analyses. Furthermore, the rats were subjected to biomarker measurements at days 7, 28, and 56. Finally, the rats were sacrificed with a sealed euthanasia device, and before that, carbon dioxide was pumped into the device, so that the rats could enter the anesthesia faster with reduced fear and pain. Then the lung specimens were harvested and processed for the subsequent analyses. Furthermore, the rats were subjected to biomarker measurements at days 7, 28, and 56.

Drug

The rhCygb was produced according to the method described previously [20]. It was dissolved in phosphate buffer saline and administered at 4 mg/kg subcutaneously. The selection of this dose of rhCygb was based on one of our previous studies [20].

Computed tomography analysis

Seven days after the BLM treatment, CT scans were performed to assess the BLM-induced changes in lung density. The rats were scanned at 7 and 56 days postoperatively. The rats were placed in a prone position, under 2% vol. isoflurane anesthesia, and then they underwent plain CT scans with multi-slice spiral CT (SOMATOM Emotion 16, Siemens, Erlangen, Ger-

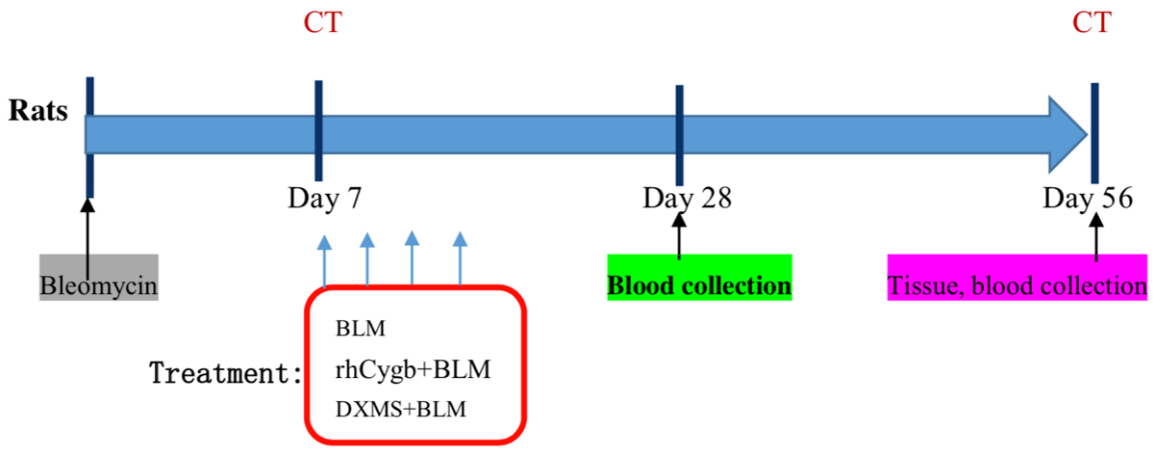

Figure 1. Schematic diagram of the experimental design. The rats were intratracheally injected with BLM. Seven days later, their CT and biomarkers were measured to confirm the establishment of lung fibrosis in the rats. Then the BLM-treated rats were divided into the BLM, rhCygb+BLM (4 mg/kg, daily, s.c.) and DXMS+BLM (3 mg/kg, daily, s.c.) groups. Blood samples were collected at days 7, 28, and 56. Finally, the rats were sacrificed and the parameters were studied.

many). The plain CT scan conditions were as follows: 80 kV with 500 μA, a pitch of 0.7 mm, a slice thickness of 0.7 mm, and an acquisition time of 32 s, 512×512 matrix, FOV 9.6 cm, and 1000 projections per scan. The images were reconstructed and analyzed. The mean lung density (MLD) for the entire lung volumes for each rat was calculated using Somaris/5VB-10B software. The MLD was assessed using the quantitative determination of the overall lung Hounsfield units (Hu) [25]. Before scanning, the MLD for air was calibrated as -1000, and the water was calibrated as 0.

Histological assessment of the lung injuries

At day 56, the rats were sacrificed after the CT scans were performed and the lungs were carefully isolated for the histological analyses. The lungs were fixed with neutral buffered formalin (10%), dehydrated and embedded in paraffin, and then sectioned at 5 μm thickness. The slices were stained with hematoxylin and eosin (H&E) and Masson trichrome staining (Sigma-Aldrich, Saint Louis, Unite States), and observed under a microscope (Seepack TX510, Shenzhen, China) for assessing the lung injuries. Masson trichrome staining was performed to detect left lung fibrosis. Four fields of each sample were randomly selected, and the collagen volume fractions (CVF) were assessed using Image-Pro Plus 6.0 to represent the degree of fibrosis in the left lung. CVF (%) refers to the percentage of the area stained positive for collagen relative to the total area in a field of view [26].

Hydroxyproline content

To obtain a quantitative measure of the lung collagen at the end of the 56 days, hydroxyproline, the major component of collagen, was measured in the lung tissues using Hydroxyproline Assay Kits (Nanjing Jiancheng Bioengineering Institute, Nanjing, China). After euthanizing the rats and harvesting the lung tissue, 30-60 mg (wet weight) of tissue was taken and put into glass vials. One ml hydrolysate was added to each vial, then the vials were capped tightly and hydrolyzed at 60°C for 20 min. The hydrolysate was then centrifuged at 3500 rpm for 10 min according to the instructions of the HYP assay kits. The absorbance was measured at 560 nm using a spectrophotometer, and the HYP content of the lung tissue was calculated according to the kit manufacturer's protocol.

Measurement of the serum HA, LN, PIIINP, and IVC levels

On days 7, 28, and 56, blood samples were collected from the veil, and the serum was separated using centrifugation at 4°C and stored at -20°C for future use. The serum HA, LN, PIIINP, and IVC levels were determined using a chemiluminescence immunoassay kit (Shenzhen New Industry Biomedical Engineering Ltd., Shenzhen, China) according to the instructions

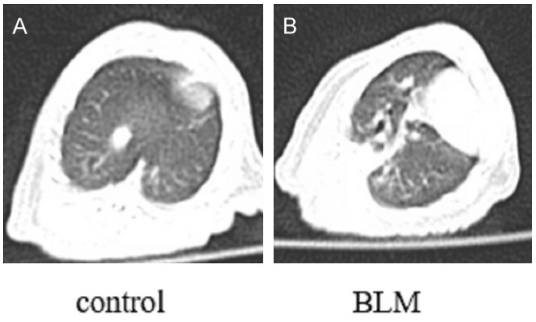

Figure 2. Computed tomography images of the control rats (A) and the BLM-treated rats (B). (A) normal findings on a CT image at day 7 after the intratracheal saline instillation. (B) peribronchial wall thickening, consolidation and ground glass attention on a CT image at day 7 after the intratracheal BLM instillation.

and using an automatic chemiluminescence analyzer (Shenzhen New Industry Biomedical Engineering Ltd., Shenzhen, China).

Statistical analysis

The statistical analysis was performed using the statistical analysis software GraphPad Prism 7 (GraphPad Software, San Diego, CA). The experimental results were given as the mean ± standard errors of the mean. The group comparisons were performed using one-way or two-way ANOVA followed by Bonferroni post hoc multiple comparison tests. The correlations of the serum LN, IVC, PIIINP, and HA levels with the CT scores were analyzed using bivariate linear regressions. The results were considered statistically significant at $P<0.05$.

Results

Establishment of the BLM-induced pulmonary fibrosis model in the rats

CT is a routine, rapid, and non-invasive method for the diagnosis and characterization of IPF [27]. To evaluate the BLM-induced rat model at day 7, CT was used to analyze the marked changes in the lungs. Compared to the control rats, the lungs of the BLM-treated rats indicated a parenchymal opacity, with the main features of a peripheral, predominantly basal pattern of coarse reticulation (**Figure 2**). Moreover, the CT MLD for the BLM-treated rats was -(704.78±19.76) Hu (n=11), and for the control rats, the MLD was -(401.71±22.29) Hu (n=34) (**Table 1**). The ECM molecules, including LN, IVC, PIIINP, and HA, are the main components of lung collagen and are associated with pulmonary fibrosis [28-30]. The serum LN, IVC, PIIINP, and HA levels in the BLM-treated rats were significantly increased compared with the control rats, specifically, 103.69±6.27 vs 70.84±2.70 of LN; 421±12.73 vs 305.61±49.42 of IVC; 106.55±4.91 vs 71.21±10.45 of PIIINP; 668.36±63.3 vs 411.26±225.73 of HA, all $P<0.001$. See **Table 1**. Together with the CT results, the data showed that the IPF rat model was well established.

rhCygb reversed the BLM-induced histopathological and fibrotic changes in the lungs

We explored the effect of rhCygb on the histopathological and fibrotic changes in the lungs induced by BML. In **Figure 3A**, the CT scan images at day 56 show the differences in the fibrotic and non-fibrotic lungs in the BLM-treated and control groups, while rhCygb had improved the lung architecture with observable reduced collage deposition and a loss of air spaces. The rats that received DXMS also had an observable effect on their lungs compared to the BLM-treated rats.

Morphologically, compared with the smooth surfaces of the control lungs, the BLM-treated rats had rough, ugly surfaces on their lungs which had gray fibrous nodules. On the other hand, the rhCygb clearly improved the pulmonary morphology in the rats which had no fibrous nodules (**Figure 3B**).

The H&E staining showed normal lung tissue structures and intact alveolar cavities in the control group. In the BLM-treated group, there was significant alveolar cavity collapse. The alveolar septum, deposition with hemoglobin, was thickened. The alveolar septum was less thickened in the rhCygb+BLM and DXMS+BLM groups (**Figure 3C**).

Masson trichrome staining (**Figure 3D**) revealed that the lung tissues in the control group had no obvious fibroblast foci. In the BLM-treated group, the BLM enhanced the pulmonary alveolus inflammation and broadened the alveolar septa. Moreover, there was a lot of collagen deposition in the lung tissue and the pulmonary fibrosis was severe. In the rhCygb and DXMS treatment groups, the alveolar wall was less thickened and the inflammatory cell infil-

Table 1. Comparison and correlation of the serum HA, LN, PIIINP, and IVC to CT MLD levels ($\bar{x}$ ± SEM)

Group	n	HA (ng/mL)	LN (ng/mL)	PIIINP (ng/mL)	IVC (ng/mL)	MLD (Hu)
Control	11	411.26±225.73	70.84±2.70	71.21±10.45	305.61±49.42	-(704.78±19.76)
BLM	34	668.36±63.30***	103.69±6.27***	106.55±4.91***	421±12.73***	-(401.71±22.29)***

HA = and hyaluronic acid, LN = laminin, PIIINP = procollagen III N-terminal peptide; IVC = type IV collagen, MLD = Mean lung density. Compared with the control group ***P<0.001.

tration was decreased. Additionally, there were decreased fibroblasts in the lung tissues. However, microthrombi were found in the bronchi of the DXMS treatment group, compared to the control group. The Masson CVF results (**Figure 3E**) showed that the average percentage of lung fibrosis in the control group was 1.86±1.51%. In contrast, the rats treated with BLM had higher levels of lung fibrosis, which was 40.33±2.08%. In the rhCygb and DXMS treatment groups, the CVFs were 20.81± 1.65% and 30.76±1.57%, respectively. The comparisons between each group were statistically significantly different (the control group vs the BLM group, P<0.001; the BLM group vs the rhCygb+BLM group, P<0.001; the BLM group vs the DXMS+BLM group, P<0.001).

The hydroxyproline levels in the lung tissue of the BLM-treated group (1.07±0.03 μg/mL) were significantly higher than the corresponding levels in the control group (0.77±0.06 μg/mL) (P<0.05). In the rhCygb and DXMS treatment groups, the HYP levels were significantly lower than they were in the BLM group, specifically 0.84±0.01 μg/mL and 0.94±0.02 μg/mL (P< 0.05). See **Figure 3F**. This result was consistent with the Masson staining results.

The CT MLD acquired by the experiments is shown in **Figure 3G**. Since most parts of the lungs are composed of air, the MLD of the control lungs tends towards -800 Hu. The CT MLD in the BLM-treated group -(404.75±20.13) Hu was significantly higher than it was in the control group -(704.78±15.13) Hu (P<0.001). In the rhCygb and DXMS treatments, the CT MLD levels were significantly lower than they were in the BLM group, respectively -(572.39±19.45) Hu and -(520.67±26.4) Hu (P<0.001).

The effect of rhCygb on the serum HA, LN, PIIINP and IVC levels

The HA, LN, PIIINP, and IVC levels in the rats at days 7, 28, and 56 were measured using the blood corresponding to the CT analysis in **Figure 4**. With a longer process of fibrosis, the HA, LN, PIIINP and IVC levels increased from 7 days to 56 days. The serum HA, LN, PIIINP and IVC levels in the BLM-treated group were approximately 2.14, 1.61, 1.69, and 1.48 folds of those in the controls, respectively (all P<0.001). Both the rhCygb and the DXMS significantly reduced the HA, LN, PIIINP and IVC levels in the blood of the pulmonary fibrosis rats (P<0.001). And at day 56, there was no significant difference in the HA, LN, or PIIINP levels between the rhCygb and the control groups except in the IVC levels (*P*>0.1).

Correlation of the serum HA, LN, PIIINP, and IVC levels and the HYP and CVF to CT MLD levels

Positive correlations were observed between the CT MLD and the LN, IVC, PIIINP, and HA levels, and HYP and CVF (**Figure 5**). The HA, LN, PIIINP and IVC levels exhibited moderate correlations with the CT MLD (R^2=0.4103, P<0.001; R^2=0.627, P<0.001; R^2=0.6995, P<0.001; R^2= 0.7489, P<0.001; respectively). The HYP also showed a moderate correlation with the CT MLD (R^2=0.7127, P<0.001). Masson CVF (%) showed very strong correlations with CT MLD (R^2=0.9376, P<0.001).

Discussion

The establishment of a BLM-induced lung fibrosis model

The BLM-induced lung fibrosis model has played a pivotal role in the search for antifibrotic agents for treating pulmonary fibrosis [31]. An *Official American Thoracic Society Workshop Report* confirmed that there was a consensus of opinion describing the intratracheal BLM model as “the best-characterized animal model available for preclinical testing” [32]. Nevertheless, sex and age differences in mice might affect the experimental results. Young mice, aged 8-12 weeks, have been reported to undergo a spontaneous resolution of BLM-induced pulmonary fibrosis, but this phenomenon does

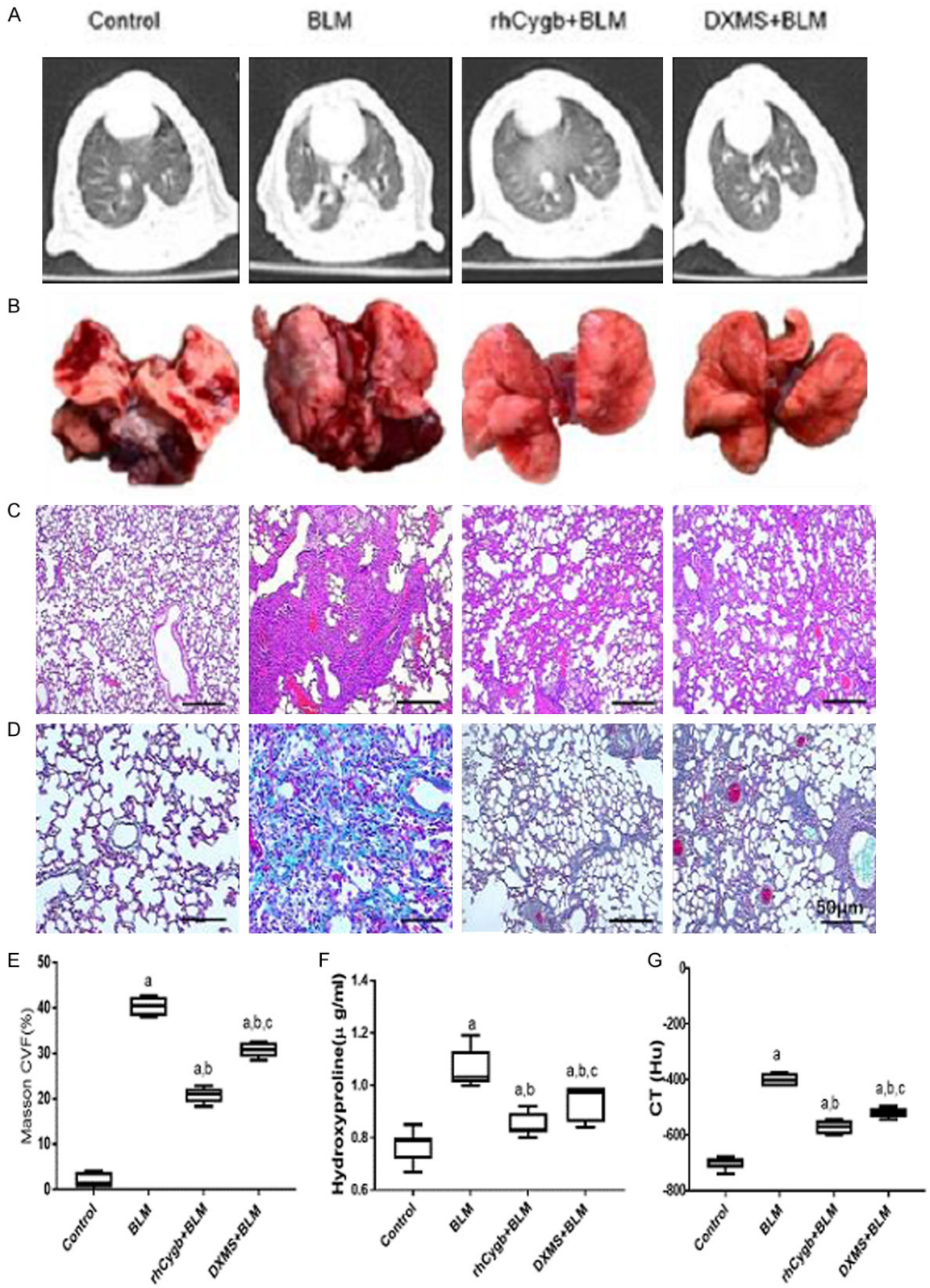

Figure 3. A morphological and histological analysis of the lungs at day 56 after the administration of treatments. A. Representative images of CT between the different treatment groups. The BLM-treated rats show diffuse peribronchial wall thickening and ground glass opacity in their lungs. B. Representative images showing the gross lung morphology of the rats. C. Representative photomicrographs of the lung sections stained with H&E (200×). D. Rep-

resentative images of the lung sections stained with Masson trichrome (200×). E. The collagen volume fractions of the lung. The data represents the mean ± SEM; n=7-11 per group. F. Hydroxyproline content. The data represents the mean ± SEM; n=7-11 per group. G. Mean lung density of CT. The data represents the mean ± SEM; n=7-11 per group. Note: [a]compared with the control group (P<0.001); [b]compared with the BLM group (P<0.001); [c]compared with the rhCygb+BLM group (P<0.001).

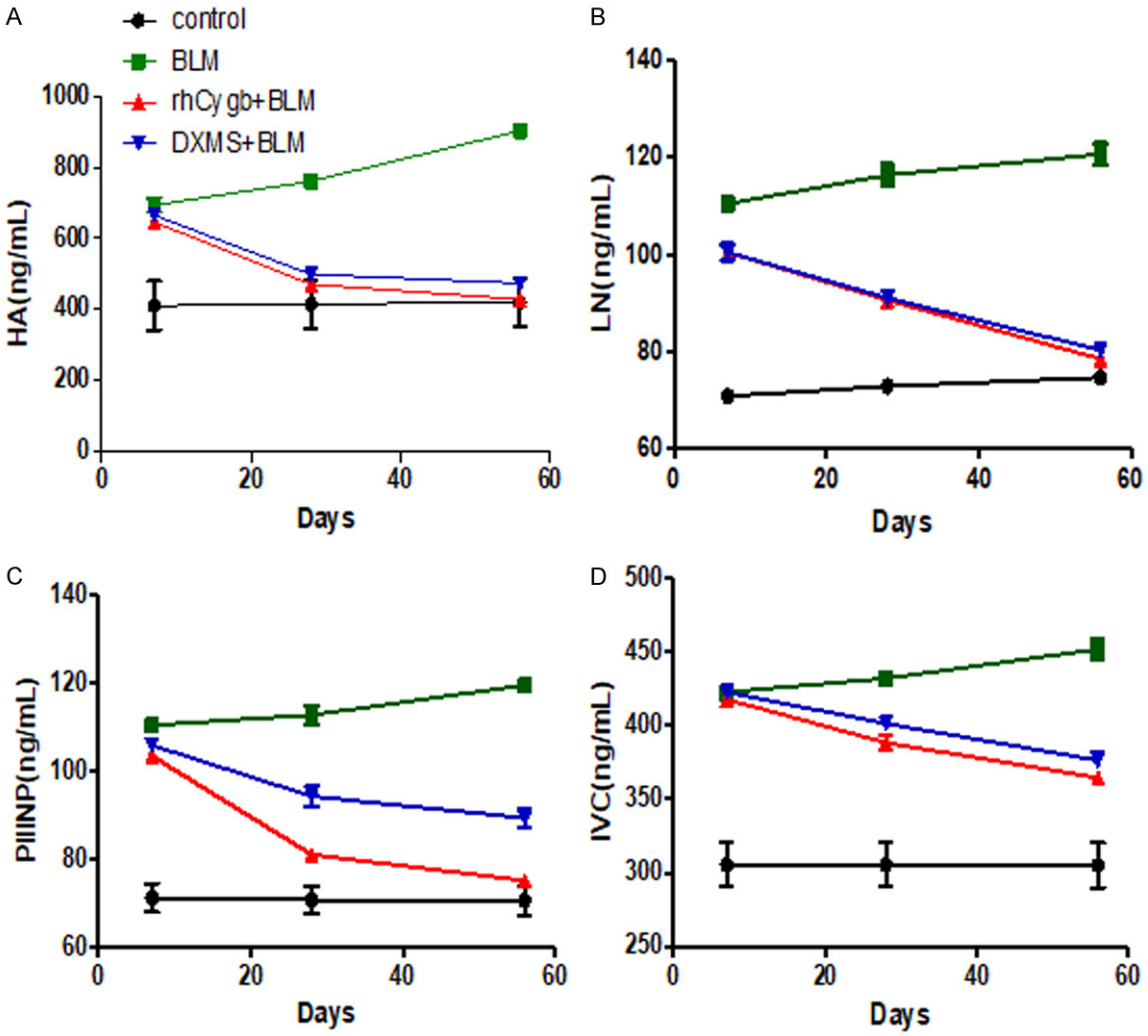

Figure 4. Effect of the rhCygb on the rats' serum HA, LN, PIIINP and IVC level. The serum HA (A), LN (B), PIIINP (C), and IVC levels (D) at days 7, 28, and 56 were analyzed in the control, BML, rhCygb+BLM, and DXMS+BLM groups. Shown are the concentrations of HA, LN, PIIINP and IVC from at least 3 experiments. HA = and hyaluronic acid, LN = laminin, PIIINP = procollagen III N-terminal peptide; IVC = type IV collagen.

not occur in aged mice [33]. Thus, aged male mice are recommended for experimental research, which may provide a more clinically relevant IPF model. In our study, adult male SD rats were used in the BLM-induced pulmonary fibrosis model.

Recently, some researchers pointed out that therapies are usually administered within <7 days following the BLM exposure, which may represent a stage of inflammation or early fibrosis, so the therapeutic effects may cause a prevention of the inflammatory cascade rather than a reversal of the fibrosis, and this is in contrast to the clinical situation when the fibrosis has already been established [34]. Thus, more recent studies have begun to explore the administration of drugs after 7 days [35, 36]. However, those papers were based on the hypothesis that the lung fibrosis was induced 3 or 4 weeks after bleomycin instillation without diagnosing the establishment of a lung fibrosis

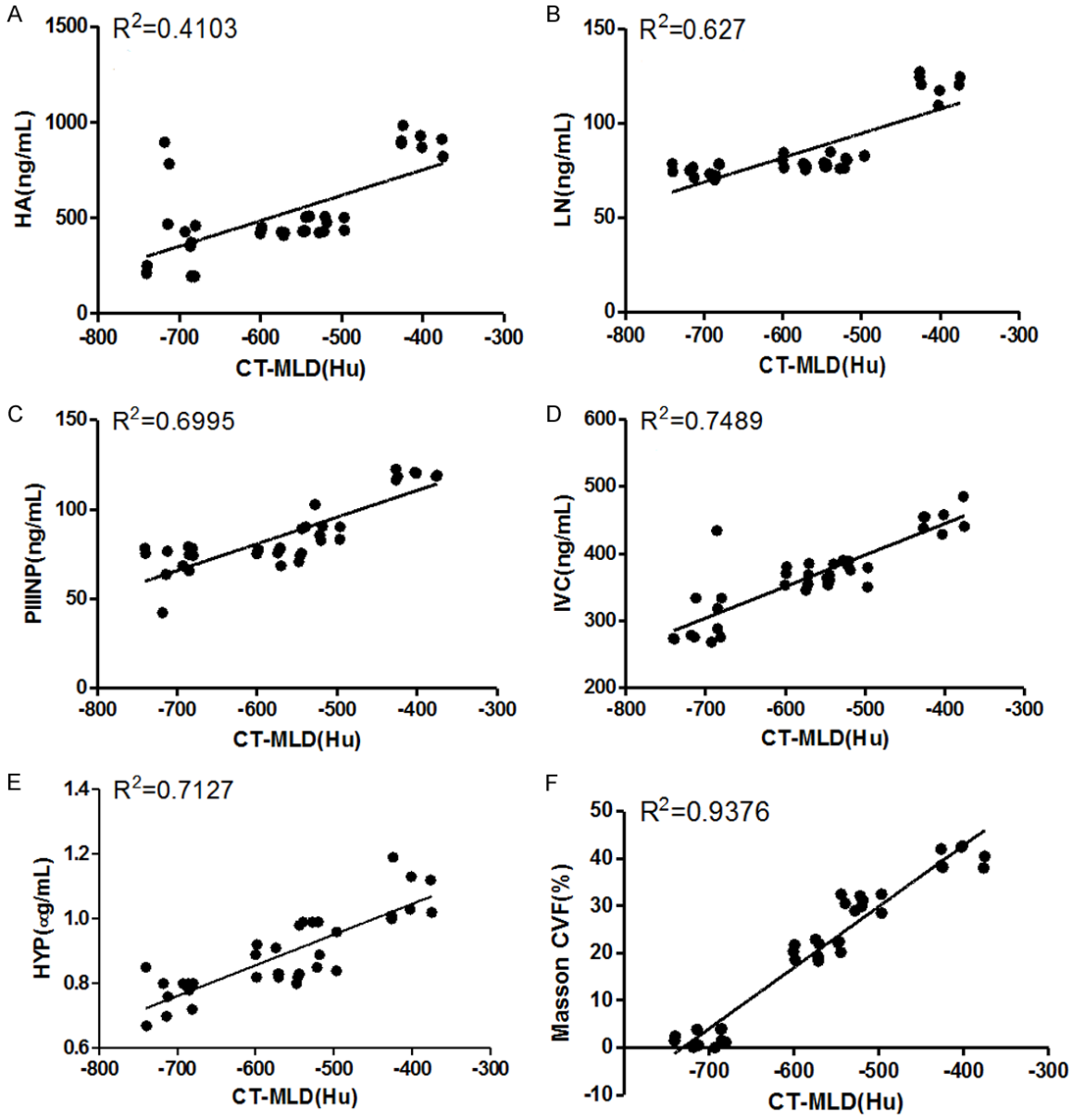

Figure 5. Correlations of the serum HA (A), LN (B), PIII NP (C), IVC (D), HYP (E), and Masson CVF (F) levels compared with the CT MLD in the experimental rats, including the control, BLM, rhCygb+BLM and DXMS+BLM groups. HA = and hyaluronic acid, LN = laminin, PIIINP = procollagen III N-terminal peptide; IVC = type IV collagen. MLD = Mean lung density, HYP = hydroxyproline, CVF = collage volume fraction.

model. Surprisingly, Choi reported that more than half of the bleomycin-instilled mice did not show lung fibrosis at 3 weeks or even 6 weeks using micro-CT [37]. So it is very essential to develop assessment methods or tools for the establishment of IPF animal models. CT is used to evaluate the IPF as a non-invasive technique in humans, with the feature of honeycombing or traction bronchiectasis and a reticular abnormality consistent with fibrosis present in a basal and peripheral predominance [38]. Until now, with increasing technical possibilities, micro-CT provides high-resolution anatomical images of small animals, and it allows repeated measurements, which avoid animal euthanasia [37, 39]. Interestingly, in our study, we confirmed that a fibrotic phase in the BLM-induced fibrosis model has been well established at 7 days using spiral CT, showing alveolar septal thickening, interstitial fibrosis, and honeycomb-

ing. This may be due to the animal breed, gender, dose, and administration affecting the results. Peng reported that bleomycin induced a dose-dependent increase in lung fibrosis, and significant fibrosis was observed in the groups of mice with higher dose [40]. These observations would support our hypothesis that testing of candidate drugs (rhCygb or DXMS) during the stage of late fibrosis is likely to translate into a clinical therapeutic benefit, evidence that comes from the clinical situation in which the treatment is initiated after the onset of symptoms and when the fibrosis has already been established.

Furthermore, the combination of the clinical parameters and biological markers has been studied in order to achieve more accurate results regarding the prognosis of IPF. Finding biomarkers for IPF has been a central challenge for a long time and would aid the fulfillment of the need for the noninvasive diagnosis of patients with IPF. Yiliang et al. investigated the serum HA, LN, PIIINP, and IVC levels in 323 patients and 160 healthy controls and found that the serum HA, LN, PIIINP, and IVC levels were all significantly higher in the patients with IPF than in the control groups and had a significant positive association with the HRCT scores in patients with IPF [9]. However, to determine whether the serum HA, LN, PIIINP and IVC levels can reflect the development and progression of IPF, serial measurements of the serum HA, LN, PIIINP, and IVC levels at the different disease stages are required. In this study, we tested the elevation of the serum HA, LN, PIIINP, and IVC levels at 7, 28, and 56 days in the same rats in the BLM-treated group when the lung fibrosis had clearly occurred. Surprisingly, compared with the progressive serum HA, LN, PIIINP, and IVC levels, the CT MLD of the BLM-treated rats at 56 days were almost equal to their levels at 7 days. Hence, we believe it is necessary to assess the progress of fibrosis in the BLM-induced fibrosis model using CT combined with biomarker measurement.

Reversed effect of rhCygb on BLM-induced lung fibrosis

Although we have previously reported that rhCygb displays antioxidative, anti-inflammatory, and antifibrotic properties in vitro and in the animal models of liver fibrosis [20-23], its efficacy against the pulmonary fibrosis in BLM-induced rats has never been studied. Herein, we tested the candidate drugs (rhCygb and DXMS) using a well-established pulmonary fibrosis rat model made evident using CT diagnosis combined with biomarker measurement including HA, LN, PIIINP, and IVC.

In the current study, we found that rats treated with rhCygb had more improved lung architecture than the BLM-treated group, with observable reduced collage deposition and loss of air spaces in the CT imaging, and the CT MLDs were significantly lower than they were in the BLM group. It is known that CT MLD can provide a prognostic estimation of disease severity in patients with IPF and other ILDs, and high MLD values may indicate severe IPF [25]. Consistent with these beneficial effects of rhCygb (4 mg/kg) treatment in our lung fibrosis rats, we found a marked attenuation of the serum HA, LN, PIIINP and IVC levels and the HYP concentrations in the rat lungs compared to the BLM-treated rats.

Recent advances targeting ECM production and repair have provided novel approaches that could be used to treat chronic lung diseases. The ECM basement membrane matrix is composed of nonfibrillar collagens (e.g., collagens IV and V), LN, and proteoglycans, and the lungs' interstitial connective tissue is composed of complex networks of fibrillar collagen (e.g., collagens I and III) as well as HA and proteoglycans. The excessive accumulation of ECM molecules within the interstitial matrix is thought to underlie the pathogenesis of IPF [41, 42]. In clinical research, the serum LN, IVC, PIIINP, and HA levels were significantly increased in the patients (323 patients) with IPF or CTD-ILD compared with the healthy controls. After the treatment, the surviving patients had significantly lower serum LN, IVC, PIIINP, and HA levels than the dead patients [9]. In the current study, we found there was no significant difference in the HA, LN, PIIINP levels between the rhCygb+BLM group and the control group at 56 days, so we inferred that the reversing effect of rhCygb may be involved in the regulation of the ECM turnover.

The pathogenesis in IPF is not fully understood, but previous evidence suggests that oxidative stress, the inflammatory response, and a series of cytokines and their related signal transduc-

tion pathways are involved in this pathological process and eventually lead to disorders characterized by excessive ECM deposition, like IPF [3]. Since Cygb is well-known for its anti-oxidative and anti-inflammatory effects [19], we infer that the possible mechanism underlying the reversing effect of rhCygb in lung fibrosis may be achieved by regulating oxidative stress and inflammation. Regardless, this will require further study.

In conclusion, we demonstrate that in addition to the effect of reversing lung fibrosis, rhCygb can reduce the serum HA, LN, Col III, and Col IV levels, indicating that it has definite effects in the regulation of ECM turnover. Since targeting ECM production provides novel approaches to treating chronic lung diseases, rhCygb could be a novel candidate drug for the development of lung fibrosis therapies.

Acknowledgements

This work was supported by a grant from the Guangzhou Science and Technology Plan Project: Major Project of Collaborative Innovation of Industry, University and Research (No. 2016-04046010), a grant from the Guangdong Province Science and Technology Plan Project (No. 2013A022100027), and a grant from the Guangzhou Science and Technology Project (No. 201804010046).

Disclosure of conflict of interest

None.

Address correspondence to: Wenqi Dong, Laboratory Medicine and Biotechnology, Southern Medical University, Guangzhou 510515, Guangdong Province, PR China. Tel: +86-20-61648556; Fax: +86-20-61648556; E-mail: dongwq63@263.net

References

[1] Martinez FJ, Collard HR, Pardo A, Raghu G, Richeldi L, Selman M, Swigris JJ, Taniguchi H and Wells AU. Idiopathic pulmonary fibrosis. Nat Rev Dis Primers 2017; 3: 17074.

[2] Raghu G, Collard HR, Egan JJ, Martinez FJ, Behr J, Brown KK, Colby TV, Cordier JF, Flaherty KR, Lasky JA, Lynch DA, Ryu JH, Swigris JJ, Wells AU, Ancochea J, Bouros D, Carvalho C, Costabel U, Ebina M, Hansell DM, Johkoh T, Kim DS, King TE Jr, Kondoh Y, Myers J, Müller NL, Nicholson AG, Richeldi L, Selman M, Dudden RF, Griss BS, Protzko SL and Schünemann HJ; ATS/ERS/JRS/ALAT Committee on Idiopathic Pulmonary Fibrosis. An official ATS/ERS/JRS/ALAT statement: idiopathic pulmonary fibrosis: evidence-based guidelines for diagnosis and management. Am J Respir Crit Care Med 2011; 183: 788-724.

[3] Barratt SL, Creamer A, Hayton C and Chaudhuri N. Idiopathic pulmonary fibrosis (IPF): an overview. J Clin Med 2018; 7: 201.

[4] Calabrese F, Giacometti C, Lunardi F and Valente M. Morphological and molecular markers in idiopathic pulmonary fibrosis. Expert Rev Respir Med 2008; 2: 505-20.

[5] Theocharis AD, Skandalis SS, Gialeli C and Karamanos NK. Extracellular matrix structure. Adv Drug Deliv Rev 2016; 97: 4-27.

[6] White ES. Lung extracellular matrix and fibroblast function. Ann Am Thorac Soc 2015; 12 Suppl 1: S30-33.

[7] Morales-Nebreda LI, Rogel MR, Eisenberg JL, Hamill KJ, Soberanes S, Nigdelioglu R, Chi M, Cho T, Radigan KA, Ridge KM, Misharin AV, Woychek A, Hopkinson S, Perlman H, Mutlu GM, Pardo A, Selman M, Jones JC and Budinger GR. Lung-specific loss of α3 laminin worsens bleomycin-induced pulmonary fibrosis. Am J Respir Cell Mol Biol 2015; 52: 503-12.

[8] Teles-Grilo ML, Leite-Almeida H, Martins dos Santos J, Oliveira C, Boaventura P and Grande NR. Differential expression of collagens type I and type IV lymphangiogenesis during the angiogenic process associated with bleomycin-induced pulmonary fibrosis in rat. Lymphology 2005; 38: 130-5.

[9] Su Y, Gu H, Weng D, Zhou Y, Li Q, Zhang F, Zhang Y, Shen L, Hu Y and Li H. Association of serum levels of laminin, type IV collagen, procollagen III N-terminal peptide, and hyaluronic acid with the progression of interstitial lung disease. Medicine (Baltimore) 2017; 96: e6617.

[10] Kawada N, Kristensen DB, Asahina K, Nakatani K, Minamiyama Y, Seki S and Yoshizato K. Characterization of a stellate cell activation-associated protein (STAP) with peroxidase activity found in rat hepatic stellate cells. J Biol Chem 2001; 276: 25318-23.

[11] Tejero J, Kapralov AA, Baumgartner MP, Sparacino-Watkins CE, Anthonymutu TS, Vlasova II, Camacho CJ, Gladwin MT, Bayir H and Kagan VE. Peroxidase activation of cytoglobin by anionic phospholipids: mechanisms and consequences. Biochim Biophys Acta 2016; 1861: 391-401.

[12] De Backer J, Razzokov J, Hammerschmid D, Mensch C, Hafideddine Z, Kumar N, van Raemdonck G, Yusupov M, Van Doorslaer S, Johannessen C, Sobott F, Bogaerts A and Dewilde S.

The effect of reactive oxygen and nitrogen species on the structure of cytoglobin: a potential tumor suppressor. Redox Biol 2018; 19: 1-10.
[13] Bosselut N, Housset C, Marcelo P, Rey C, Burmester T, Vinh J, Vaubourdolle M, Cadoret A and Baudin B. Distinct proteomic features of two fibrogenic liver cell populations: hepatic stellate cells and portal myofibroblasts. Proteomics 2010; 10: 1017-28.
[14] Xu R, Harrison PM, Chen M, Li L, Tsui T-Y, Fung PCW, Cheung P-T, Wang G, Li H, Diao Y, Krissansen GW, Xu S and Farzaneh F. Cytoglobin overexpression protects against damage-induced fibrosis. Mol Ther 2006; 13: 1093-100.
[15] Mimura I, Nangaku M, Nishi H, Inagi R, Tanaka T and Fujita T. Cytoglobin, a novel globin, plays an anti-fibrotic role in the kidney. Am J Physiol Renal Physiol 2010; 299: F1120-33.
[16] Thuy le TT, Matsumoto Y, Thuy TT, Hai H, Suoh M, Urahara Y, Motoyama H, Fujii H, Tamori A, Kubo S, Takemura S, Morita T, Yoshizato K and Kawada N. Cytoglobin deficiency promotes liver cancer development from hepatosteatosis through activation of the oxidative stress pathway. Am J Pathol 2015; 185: 1045-60.
[17] Yassin M, Kissow H, Vainer B, Joseph PD, Hay-Schmidt A, Olsen J and Pedersen AE. Cytoglobin affects tumorigenesis and the expression of ulcerative colitis-associated genes under chemically induced colitis in mice. Sci Rep 2018; 8: 6905.
[18] Latina A, Viticchiè G, Lena AM, Piro MC, Annicchiarico-Petruzzelli M, Melino G and Candi E. ΔNp63 targets cytoglobin to inhibit oxidative stress-induced apoptosis in keratinocytes and lung cancer. Oncogene 2016; 35: 1493-1503.
[19] Oleksiewicz U, Liloglou T, Field JK and Xinarianos G. Cytoglobin: biochemical, functional and clinical perspective of the newest member of the globin family. Cell Mol Life Sci 2011; 68: 3869-83.
[20] Li Z, Wei W, Chen B, Cai G, Li X, Wang P, Tang J and Dong W. The Effect of rhCygb on CCl4-induced hepatic fibrogenesis in rat. Sci Rep 2016; 6: 23508.
[21] Wen J, Wu Y, Wei W, Li Z, Wang P, Zhu S and Dong W. Protective effects of recombinant human cytoglobin against chronic alcohol-induced liver disease in vivo and in vitro. Sci Rep 2017; 7: 41647.
[22] Cai G, Chen B, Li Z, Wei W, Wang P and Dong W. The different expressed serum proteins in rhCygb treated rat model of liver fibrosis by the optimized two-dimensional gel electrophoresis. PLoS One 2017; 12: e0177968.
[23] Ou L, Li X, Chen B, Ge Z, Zhang J, Zhang Y, Cai G, Li Z, Wang P and Dong W. Recombinant human cytoglobin prevents atherosclerosis by regulating lipid metabolism and oxidative stress. J Cardiovasc Pharmacol Ther 2018; 23: 162-173.
[24] Chen L, Wang T, Wang X, Sun BB, Li JQ, Liu DS, Zhang SF, Liu L, Xu D, Chen YJ and Wen FQ. Blockade of advanced glycation end product formation attenuates bleomycin-induced pulmonary fibrosis in rats. Respir Res 2009; 10: 55.
[25] Zhou C, Jones B, Moustafa M, Schwager C, Bauer J, Yang B, Cao L, Jia M, Mairani A, Chen M, Chen L, Debus J and Abdollahi A. Quantitative assessment of radiation dose and fractionation effects on normal tissue by utilizing a novel lung fibrosis index model. Radiat Oncol 2017; 12: 172.
[26] Liu Q, Song J, Lu D, Geng J, Jiang Z, Wang K, Zhang B and Shan Q. Effects of renal denervation on monocrotaline induced pulmonary remodeling. Oncotarget 2017; 8: 46846-46855.
[27] Zhang Y, Wu X, Yang W, Feng Q and Chen W. Super-resolution reconstruction for 4D computed tomography of the lung via the projections onto convex sets approach. Med Phys 2014; 41: 111917.
[28] Balestrini JL and Niklason LE. Extracellular matrix as a driver for lung regeneration. Ann Biomed Eng 2015; 43: 568-76.
[29] Tashiro J, Rubio GA, Limper AH, Williams K, Elliot SJ, Ninou I, Aidinis V, Tzouvelekis A and Glassberg MK. Exploring animal models that resemble idiopathic pulmonary fibrosis. Front Med (Lausanne) 2017; 4: 118.
[30] Sun NN, Yu CH, Pan MX, Zhang Y, Zheng BJ, Yang QJ, Zheng ZM and Meng Y. Mir-21 mediates the inhibitory effect of ang (1-7) on AngII-induced NLRP3 inflammasome activation by targeting spry1 in lung fibroblasts. Sci Rep 2017; 7: 14369.
[31] Ni S, Wang D, Qiu X, Pang L, Song Z and Guo K. Bone marrow mesenchymal stem cells protect against bleomycin-induced pulmonary fibrosis in rat by activating Nrf2 signaling. Int J Clin Exp Pathol 2015; 8: 7752-7761.
[32] Jenkins RG, Moore BB, Chambers RC, Eickelberg O, Konigshoff M, Kolb M, Laurent GJ, Nanthakumar CB, Olman MA, Pardo A, Selman M, Sheppard D, Sime PJ, Tager AM, Tatler AL, Thannickal VJ and White ES; ATS Assembly on Respiratory Cell and Molecular Biology. An official American Thoracic Society workshop report: use of animal models for the preclinical assessment of potential therapies for pulmonary fibrosis. Am J Respir Cell Mol Biol 2017; 56: 667.
[33] Redente EF, Jacobsen KM, Solomon JJ, Lara AR, Faubel S, Keith RC, Henson PM, Downey GP and Riches DW. Age and sex dimorphisms contribute to the severity of bleomycin-induced

lung injury and fibrosis. Am J Physiol Lung Cell Mol Physiol 2011; 301: L510-8.
[34] Cross J, Stenton GR, Harwig C, Szabo C, Genovese T, Di Paola R, Esposito E, Cuzzocrea S and Mackenzie LF. AQX-1125, a small molecule SHIP1 activator, inhibits bleomycin-induced pulmonary fibrosis. Br J Pharmacol 2017; 174: 3045-3057.
[35] Tanaka KI, Niino T, Ishihara T, Takafuji A, Takayama T, Kanda Y, Sugizaki T, Tamura F, Kurotsu S, Kawahara M and Mizushima T. Protective and therapeutic effect of felodipine against bleomycin-induced pulmonary fibrosis in mice. Sci Rep 2017; 7: 3439.
[36] Lee SH, Lee EJ, Lee SY, Kim JH, Shim JJ, Shin C, In KH, Kang KH, Uhm CS, Kim HK, Yang KS, Park S, Kim HS, Kim YM and Yoo TJ. The effect of adipose stem cell therapy on pulmonary fibrosis induced by repetitive intratracheal bleomycin in mice. Exp Lung Res 2014; 40: 117-125.
[37] Choi EJ, Jin GY, Bok SM, Han YM, Lee YS, Jung MJ and Kwon KS. Serial micro-CT assessment of the therapeutic effects of rosiglitazone in a bleomycin-induced lung fibrosis mouse model. Korean J Radiol 2014; 15: 448-55.
[38] Andrade J, Schwarz M, Collard HR, Gentry-Bumpass T, Colby T, Lynch D and Kaner RJ; IPFnet Investigators. The idiopathic pulmonary fibrosis clinical research network (IPFnet): diagnostic and adjudication processes. Chest 2015; 148: 1034-1042.
[39] Rodt T, von Falck C, Dettmer S, Halter R, Maus R, Ask K, Kolb M, Gauldie J, Länger F, Hoy L, Welte T, Galanski M, Maus UA and Borlak J. Micro-computed tomography of pulmonary fibrosis in mice induced by adenoviral gene transfer of biologically active transforming growth factor-β1. Respir Res 2010; 11: 181.
[40] Peng R, Sridhar S, Tyagi G, Phillips JE, Garrido R, Harris P, Burns L, Renteria L, Woods J, Chen L, Allard J, Ravindran P, Bitter H, Liang Z, Hogaboam CM, Kitson C, Budd DC, Fine JS, Bauer CM and Stevenson CS. Bleomycin induces molecular changes directly relevant to idiopathic pulmonary fibrosis: a model for "active" disease. PLoS One 2013; 8: e59348.
[41] King TE Jr, Pardo A and Selman M. Idiopathic pulmonary fibrosis. Lancet 2011; 378: 1949-1961.
[42] Gu BH, Madison MC, Corry D and Kheradmand F. Matrix remodeling in chronic lung diseases. Matrix Biol 2018; 73: 52-63.